Chemistry of Metals and Alloys

Chem. Met. Alloys 18 (2025) 6-11
Ivan Franko National University of Lviv
http://publications.lnu.edu.ua/chemetal

Chemisorption-catalytic properties of compositions based on *d*-metal compounds and NaX zeolite in the reaction of sulfur dioxide with atmospheric oxygen

Tatyana KIOSE[1*], Tatyana RAKYTSKA[1], Olesia DANIUKINA[1], Lyudmila RASKOLA[1]

[1] *Faculty of Chemistry and Pharmacy, Odesa I.I. Mechnikov National University, Vsevolod Zmienko St. 2, 65082 Odesa, Ukraine*
* *Corresponding author. Tel.:* +38-067-7067191*; E-mail: kiose@onu.edu.ua*

Received June 2, 2025; accepted June 25, 2025
https://doi.org/10.30970/cma18.0445

The effect of the modification of synthetic NaX zeolite by transition metal chlorides (Cu(II), Mn(II), Co(II), Ni(II)) on its structure and chemisorption-catalytic activity in the oxidation of sulfur dioxide with atmospheric oxygen was investigated. X-ray diffraction revealed that the zeolite framework was preserved, and no extraneous phases were detected in the MCl$_2$/NaX compositions (M = Cu^{2+}, Co^{2+}, Mn^{2+}, Ni^{2+}). The kinetics of SO$_2$ oxidation were investigated, and the effect of the metal cation on the activity of the MCl$_2$/NaX compositions was determined. The combined use of two research methods, namely, the desorption of metal ions by water from MCl$_2$/NaX compositions and their testing in the SO$_2$ oxidation reaction with atmospheric oxygen, made it possible to determine the contribution of inner- and outer-sphere complexes to the overall activity of the samples, and to evaluate the affinity of the ions for the zeolite surface. It was found that the MnCl$_2$/NaX and CuCl$_2$/NaX samples exhibited the best protective properties, determining their potential for use in personal respiratory protection equipment.

***d*-Metals / Sulfur dioxide / Chemisorption-catalytic activity / Zeolite**

Introduction

Sulfur dioxide (SO$_2$), from natural and anthropogenic sources, is the most common toxic atmospheric pollutant. To reduce sulfur dioxide emissions, adsorption methods are employed using natural [1,2] and synthetic [3-5] zeolites, carbon materials [6], porous polymers [7], and metal-organic frameworks (MOFs) [8]. To improve the properties of the adsorbents and increase the amount of adsorbed SO$_2$, the materials are functionalized using various methods, including chemical modification of the surface with acids [1-3], transition metal ions [3,6], and amines [9].

It is known [10] that the ion-exchanged forms of zeolite M-NaX (M = K$^+$, Ca^{2+}, Mn^{2+}, Co^{2+}) change their adsorption capacity in the following sequence: K-NaX > NaX > Mn-NaX > Ca-NaX ≈ Co-NaX under the conditions C_{SO_2} = 2000 ppm (5240 mg/m^3), C_{O_2} = 5 vol.%, and T = 90°C. This means that the modification of zeolite by Ca^{2+}, Mn^{2+}, Co^{2+} leads to a negative result, while the longest breakthrough time of 100 min was observed for K-NaX. In [11], it was established that Cu^{2+}, Mn^{2+} and Co^{2+} compounds immobilized on NaX zeolite by impregnation showed a positive effect. The breakthrough time and adsorption capacity of the samples decreased in the following sequence: CuCl$_2$/NaX > MnCl$_2$/NaX > CoCl$_2$/NaX. These results were obtained using a gas-air mixture (C_{SO_2} = 150 mg/m^3, relative humidity 76%) at a temperature of 20°C. Such conditions must be applied when developing chemosorption-catalytic compositions for lightweight personal protective equipment (PPE) for respiratory organs against sulfur dioxide. The literature search showed that information on the use of synthetic zeolites modified with metal ions in the reaction of sulfur dioxide is very limited.

The aim of this work was to investigate the chemosorption-catalytic properties of MCl$_2$/NaX (M = Cu^{2+}, Mn^{2+}. Co^{2+}, Ni^{2+}) compositions in the reaction of sulfur dioxide with atmospheric oxygen at ambient temperature and high relative humidity.

Experimental

Materials. CuCl$_2$, MnCl$_2$, CoCl$_2$, and NiCl$_2$ salts of chemically pure grade (Sigma Aldrich, USA) and

zeolite NaX (TS 2163-077-05766575-99) with SiO_2/Al_2O_3 = 2.4-2.7 were used for the work, pH of the suspension was 10.97. Samples of synthetic zeolite modified with salts of transition metals were obtained by impregnation: 10 g of NaX zeolite, dried at 110°C, with an average grain size of 0.75 mm, was placed in a Petri dish and then impregnated with aqueous solutions of MCl_2 salts (M = Cu^{2+}, Co^{2+}, Mn^{2+}, Ni^{2+}) at specified concentrations. The wet sample was dried in an oven in an air atmosphere at 110°C to constant mass. The MCl_2 content in the sample was calculated per mass unit of the dry carrier.

Methods. Phase analysis was carried out using a Siemens D500 (Germany) powder diffractometer using copper radiation (Cu K_α, λ = 1.54178 Å), with a secondary beam graphite monochromator. To record the diffractograms, the test samples were thoroughly ground in an agate mortar and placed in a glass cuvette with a working volume of 2×1×0.1 cm^3.

Investigation of the chemisorption-catalytic process. A gas-air mixture (GAM) with a SO_2 concentration of 150 mg/m^3 was obtained by mixing a purified air flow and a flow of pure SO_2 in a special mixer. Initial and final sulfur dioxide concentrations were measured using a 667EKh08 electrochemical gas analyzer (made by Analitprilad, Ukraine) with a minimal detectable SO_2 concentration of 2 mg/m^3.

The dynamics of sulfur dioxide adsorption at the studied compositions were investigated in a flow-through gas thermostatic setup at 20°C, in a glass reactor with a fixed layer of sorbent sample weighing 10 g under the following conditions: $C^{in}_{SO_2}$ = 150 mg/m^3; T = 20°C; volumetric flow rate of GAM 1 l/min, sorbent grain size 0.5-1.0 mm, linear flow rate of GAM U = 4.2 cm/s, relative humidity of GAM 76%.

The amount of adsorbed SO_2 (Q_{exp}, moles) was calculated using experimental data, which are given in the coordinates $C\Delta_{SO2} - \tau$. The stoichiometric parameter $n = Q_{exp}/Q_{theor}$ was calculated taking into account the stoichiometry of the reactions according to Eqs. (1,2).

$$SO_2 + 2Cu^{2+} + 2H_2O = H_2SO_4 + 2Cu^{+} + 2H^{+} \quad (1)$$

$$2SO_3^{2-} + M^{2+} = [M(SO_3)_2]^{2-} \quad (2)$$

M = Mn^{2+}, Co^{2+}, Ni^{2+}.

To assess the protective properties of the synthetic zeolites and their modified metal salt forms, the following parameters were used: τ_0 – period of time where the dynamic adsorption curve $C^{f}_{SO_2} = 0$; τ_{MPC} – time of protective action, *i.e.* time required to reach the maximum permissible concentration, 10 mg/m^3, for the working area [12].

Desorption of Cu^{2+}, Co^{2+}, Mn^{2+}, Ni^{2+}. Desorption of metal ions from the MCl_2/NaX composistions was carried out under static conditions using the eluent H_2O at a T:P ratio of 5:100 and a temperature of 20°C for 30 minutes. The content of desorbed metal ions in the solutions was determined by atomic absorption using an atomic absorption spectrophotometer AAS-1N from the company Carl Zeiss, Jena (Germany) [13].

Results and discussion

As an example, Fig. 1a shows the diffraction pattern of a NaX zeolite sample, identified by the basic reflections at 2θ (degrees): 6.201; 15.540; 23.540; 23.452; 26.811; 31.125, which are in accordance with literature data [14]. Fixation of cupric chloride (Cu(II)) (Fig. 1b) and other salts ($MnCl_2$, $CoCl_2$, $NiCl_2$) by the impregnation method did not lead to structural changes in the zeolite framework. For the $CuCl_2$/NaX sample, the basic reflections are close to those of the original zeolite, 2θ (degrees): 6.159; 6.201; 15.503; 23.417; 26.781; 31.093. No other phases were detected in the MCl_2/NaX samples. The results correlate with the XRD data of M-NaX samples (M = K^+, Ca^{2+}, Mn^{2+}, Co^{2+}) obtained by the ion-exchange method [13].

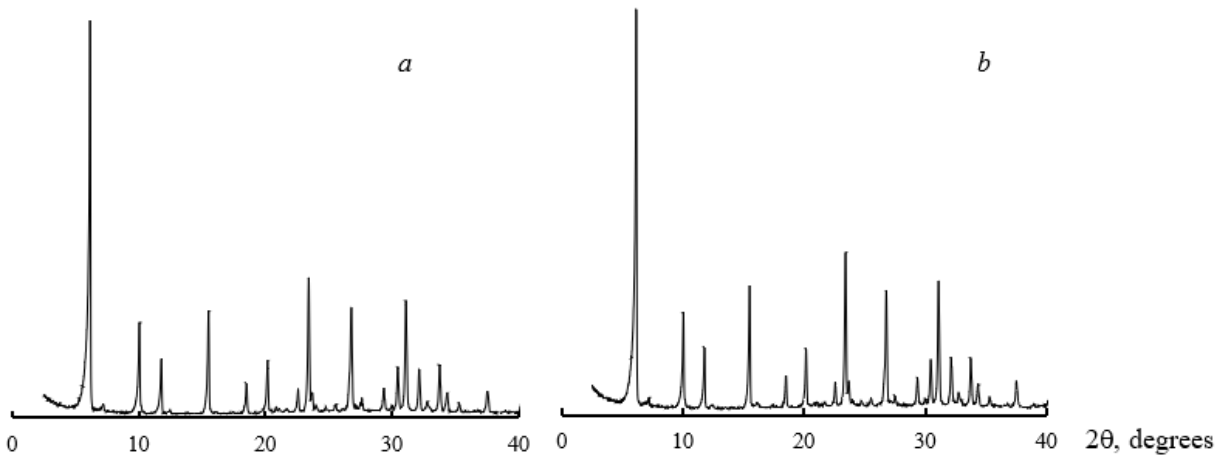

Fig. 1 X-ray diffraction patterns of the initial sample of zeolite NaX (*a*) and the sample modified with copper(II) chloride, $CuCl_2$/NaX (*b*).

Table 1 Kinetic and stoichiometric parameters of the oxidation reaction of sulfur dioxide with oxygen in the presence of zeolite NaX and MCl_2/NaX; $C^{in}_{SO_2}$ = 150 mg/m^3; $C_{M(II)}$ = 5.9×10^{-5} mol/g; U = 4.2 cm/s; T = 20°C.

Composition	τ_0, min	τ_{MPC}, min	$Q_{exp}\times10^4$, moles SO_2	$Q_{theor}\times10^4$, moles SO_2	n
NaX	230	270	7.05	–	–
$CuCl_2$/NaX	420	470	13.59	2.95	4.6
$MnCl_2$/NaX	480	580	17.35	11.80	1.5
$CoCl_2$/NaX	280	360	11.80	11.80	1.0
$NiCl_2$/NaX	180	220	5.70	11.80	0.5

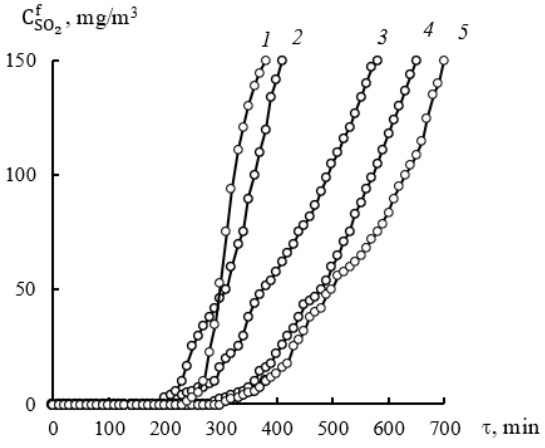

Fig. 2 Change in $C^f_{SO_2}$ over time in the process of oxidation of sulfur dioxide with oxygen in the presence of $CuCl_2$/NaX at different concentrations of copper(II) chloride: $C_{CuCl_2}\times10^5$ (mol/g): 1 – 0; 2 – 1.2; 3 – 2.9; 4 – 5.9; 5 – 11.7. $C^{in}_{SO_2}$ = 150 mg/m^3; U = 4.2 cm/s; T = 20°C.

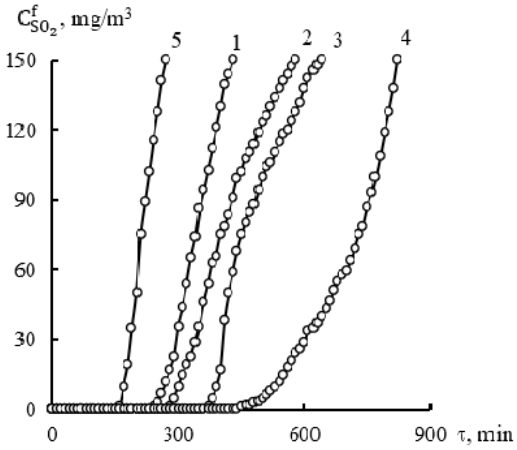

Fig. 3 Change of $C^f_{SO_2}$ over time during the oxidation of sulfur dioxide with oxygen in the presence of: 1 – NaX; 2 – $CoCl_2$/NaX; 3 – $CuCl_2$/NaX; 4 – $MnCl_2$/NaX; 5 – $NiCl_2$/NaX. $C^{in}_{SO_2}$ = 150 mg/m^3; $C_{M(II)}$ = 5.9×10^{-5} mol/g; U = 4.2 cm/s; T = 20°C.

The profiles of the kinetic curves of SO_2 adsorption by the MCl_2/NaX compositions are typical. As an example, Fig. 2 presents the results of the change in the final SO_2 concentration ($C^f_{SO_2}$, mg/m^3) in time (τ, min) when the cupric chloride content increases from 1.2×10^{-5} to 11.7×10^{-5} mol/g in the $CuCl_2$/NaX composition. For the other MCl_2/NaX compositions (M = Co^{2+}, Mn^{2+}, Ni^{2+}) the concentration was varied within the specified limits. Comparative characteristics of the activity of the compositions are given under the condition $C_{M(II)}$ = 5.9×10^{-5} mol/g (Fig. 3, Table 1). On the kinetic curves, it is possible to distinguish areas that correspond to complete adsorption of SO_2 and areas where the final concentration of SO_2 increases and reaches the initial one $C^f_{SO_2} = C^{in}_{SO_2}$. Steady-state oxidation of sulfur dioxide was observed in no case. Quantitative characteristics of the process

$$2SO_2 + O_2 + 2H_2O = 2H_2SO_4 \quad (3)$$

in the presence of MCl_2/NaX is τ_0 – time to reach SO_2 breakthrough; τ_{MPC} – time of protective action, where the final concentration of SO_2 reaches the maximum permissible concentration for the working zone (MPC_{SO_2}= 10 mg/m^3); Q_{exp} – number of SO_2 moles adsorbed in the reaction; Q_{theor} was calculated in accordance with Eqs. (1) and (2); n is the stoichiometric coefficient, which, in the case of the composition $CuCl_2$/NaX was determined taking into account reaction (1), and equation (2) for the other compositions.

The following conclusions were drawn from the analysis of the results: i) zeolite NaX directly adsorbs SO_2 and the protective effect time is 270 minutes; ii) modification of the zeolite with chlorides of Cu(II), Mn(II), or Co(II), leads to an increase of the parameters τ_0, τ_{MPC} and Q_{exp} in the sequence $MnCl_2$ > $CuCl_2$ > $CoCl_2$; iii) these parameters are, in the case of $NiCl_2$, lower than for the original zeolite; iv) the general activity series of the composition is: $MnCl_2$/NaX > $CuCl_2$/NaX > $CoCl_2$/NaX > $NiCl_2$/NaX (4); v) the value of the stoichiometric coefficient n depends on the nature of the metal ion and n > 1 in the case of Cu(II), Mn(II), which indicates catalysis of reaction (3) by these ions; vi) the process is chemisorption-catalytic, but without establishing a stationary regime. The latter fact and the low values of the stoichiometric coefficient for the compositions $CoCl_2$/NaX and $NiCl_2$/NaX may indicate blocking of the active centers of the catalyst by the reaction product, namely the sulfate ion. The course

of reaction (3) in the presence of MCl_2/NaX can be deduced based on data obtained on measuring the equilibrium pH value of the suspension according to the method described in [15]. Table 2 summarizes the pH values for the NaX and MCl_2/NaX samples before and after the reaction of SO_2 with atmospheric oxygen. In all cases, pH of the sample suspension decreases ($\Delta pH_{st} < 0$) after reaction (3), which indicates oxidation of sulfur dioxide to sulfuric acid, confirmed by a qualitative reaction with barium chloride.

Reaction (3) has been thoroughly studied in solutions in the presence of metal ions and mainly two types of mechanism were confirmed:

1. Radical mechanism, the first stage of which is the initiation of a chain:

$$M^{n+} + SO_3^{2-} \rightarrow SO_3^{\bullet -} + M^{(n-1)+}, \quad (5)$$

where $M^{n+} = Cu^{2+}$, Cu^{3+}, Fe^{3+} [16-18].

2. Non-radical two-electron mechanism by which the oxidation of SO_2 (SO_3^{2-}) by oxygen occurs intraspherically.

$$[M(SO_3)_2O_2]^{n-4} \rightarrow 2SO_4^{2-} + M^{n+}, \quad (6)$$

where $M^{n+} = Mn^{2+}$, Co^{2+}, Fe^{2+}, Ni^{2+} [19,20].

Depending on the reaction conditions and the metal ion precursors, there may be some differences in the activity series. Thus, according to [19], the following activity series was observed: $Fe^{2+} \approx Co^{2+} > Mn^{2+} \approx Cu^{1+,2+} > Fe^{3+} > Co^{3+} >> Ni^{2+}$. The sequence is somewhat different in [20]: $Cu^{2+} > Mn^{2+} > Cr^{3+}$, Fe^{3+}, Co^{2+}, Ni^{2+}, which correlates more with our results.

The course of reaction (3) in the presence of the composition MCl_2/NaX ($M = Cu^{2+}$, Mn^{2+}, Co^{2+}, Ni^{2+}) is complicated not only by various mechanisms, but also by surface complexation processes, which lead to the formation of inner-sphere (7,8) and outer-sphere (9) complexes:

$$\equiv T\text{-OH} + M^{2+} \leftrightarrow \equiv T\text{-O}M^{+} + H^{+}, \quad (7)$$

$$2\equiv T\text{-OH} + M^{2+} \leftrightarrow \equiv (T\text{-O})_2M + 2H^{+}, \quad (8)$$

$$(\equiv T\text{-O}^{-})_2 + M^{2+} \leftrightarrow (\equiv T\text{-O}^{-})_2\text{---}M^{2+}, \quad (9)$$

where T is the symbol corresponding to the tetrahedral atom of the zeolite, namely Si, Al.

Inner-sphere complexes are formed by an ion-exchange mechanism, and outer-sphere complexes are formed as a result of electrostatic interaction [21]. As our experience shows [22-24], outer-sphere complexes are easily desorbed by water even at room temperature, and the ratio of the two types of complexes is determined by the affinity of the metal ions to the surface. The formation of two types of surface complexes was confirmed by experiments on the desorption of Cu^{2+}, Mn^{2+}, Co^{2+}, Ni^{2+} ions by water at 20°C and by testing the samples in reaction (3). Fig. 4, as an example, shows the kinetics of sulfur dioxide adsorption for the initial samples $CuCl_2$/NaX (a) and $NiCl_2$/NaX (b) (curves 1) and after desorption of copper(II) and nickel(II) (curves 2). It is seen that the profile of the kinetic curves does not change, but the decrease in the reaction parameters τ_{MPC} and Q_{exp} for the desorbed samples depends on the nature of the metal ion (Table 3).

Table 2 Equilibrium pH of aqueous suspensions of NaX and MCl_2/NaX samples before and after the reaction of SO_2 with oxygen.

Sample	pH_{st}		ΔpH_{st}
	Before reaction	After reaction	
NaX	10.97	10.65	-0.32
$NiCl_2$/NaX	10.65	10.35	-0.30
$CuCl_2$/NaX	10.60	9.75	-0.85
$MnCl_2$/NaX	10.55	10.20	-0.35
$CoCl_2$/NaX	10.40	10.05	-0.35

Table 3 Results of the desorption of the metal ions for MCl_2/NaX ($M = Cu^{2+}$, Mn^{2+}, Co^{2+}, Ni^{2+}) and from testing them in the sulfur dioxide oxidation reaction; $C^{in}_{SO2} = 150$ mg/m^3; $U = 4.2$ cm/s; $T = 20$°C.

Sample	$C_M \times 10^5$, mol/g	$Q_{exp} \times 10^4$, moles SO_2	τ_{MPC}, min	Fraction of complexes, %	
				Intra-sphere	Outer-sphere
$CuCl_2$/NaX					
Initial	5.9	13,59	470	40.68	59.32
After desorption	2.4	5.37	200		
$CoCl_2$/NaX					
Initial	5.9	11.80	360	64.40	35.60
After desorption	3.8	6.93	250		
$MnCl_2$/NaX					
Initial	5.9	17.35	580	89.83	10.17
After desorption	5.3	15.40	470		
$NiCl_2$/NaX					
Initial	5.9	5.70	220	86.44	13.56
After desorption	5.1	4.95	200		

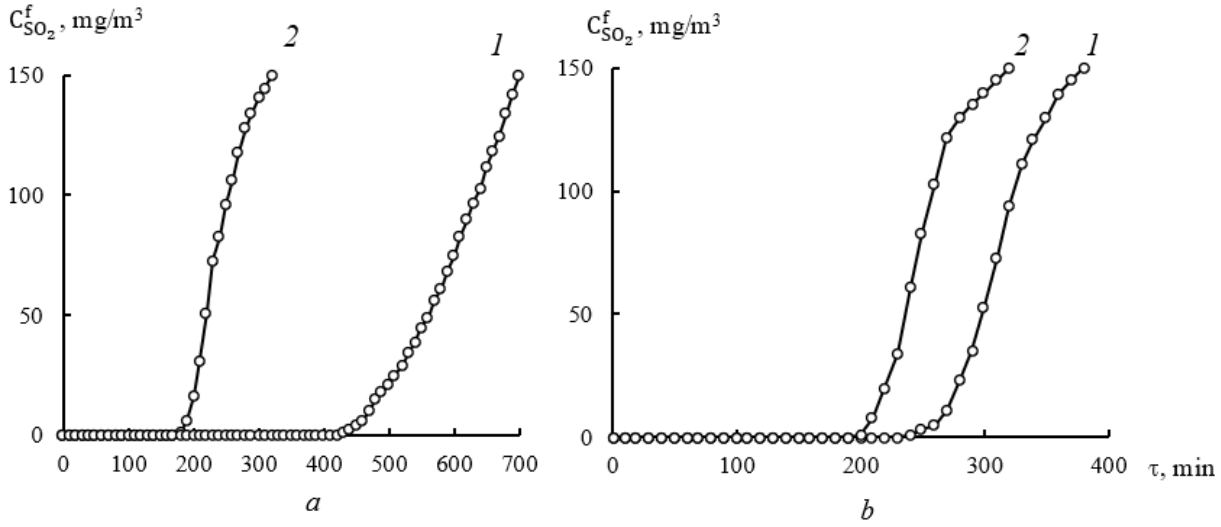

Fig. 4 Change of $C^f_{SO_2}$ over time during the oxidation of sulfur dioxide with oxygen with the initial compositions $CuCl_2$/NaX (*a*) and $NiCl_2$/NaX (*b*) (curves 1) and compositions after desorption of Cu(II) and Ni(II) (curves 2). $C^{in}_{SO_2}$ = 150 mg/m^3; $C_{M(II)} = 5.9\times10^{-5}$ mol/g; U = 4.2 cm/s; T = 20°C.

We calculated the fraction of intra-sphere and extra-sphere complexes and concluded that the affinity of metal ions to the surface of the NaX zeolite decreases in the following sequence: $Mn^{2+} > Ni^{2+} > Co^{2+} > Cu^{2+}$ (10), which does not correlate with the activity series given above (4), due to different reaction mechanisms.

Conclusions

By X-ray diffraction it was established that modification of artificial zeolite NaX with chlorides of Cu(II), Mn(II), Co(II), and Ni(II) does not affect the structure of the zeolite framework. No other phases were detected in the compositions MCl_2/NaX. It was shown that the shapes of the kinetic curves characterizing the oxidation of sulfur dioxide by air oxygen over time are identical for the original and modified samples of zeolite NaX. The process parameters, the breakthrough time of SO_2, the time of protective action, the amount of SO_2 reacted and the stoichiometric coefficient depend on the nature of the metal ion, the activity of which decreases in the following sequence: $MnCl_2$/NaX > $CuCl_2$/NaX > $CoCl_2$/NaX > $NiCl_2$/NaX (**I**). The combination of two methods, namely the desorption of metal ions with water from the MCl_2/NaX compositions and testing of the compositions in the oxidation of SO_2 by air oxygen, made it possible to calculate the proportion of inner-sphere and outer-sphere surface complexes, determine their contribution to the activity of the compositions and assess the affinity of the ions to the zeolite surface: $Mn^{2+} > Ni^{2+} > Co^{2+} > Cu^{2+}$ (**II**). One of the reasons for the discrepancy between the series (**I**) and (**II**) is the different mechanisms of SO_2 oxidation by oxygen in the presence of $CuCl_2$/NaX and the other MCl_2/NaX compositions ($M = Mn^{2+}$, Co^{2+}, Ni^{2+}). The $MnCl_2$/NaX and $CuCl_2$/NaX compositions showed the longest protective effect time and are promising for use in equipment protecting the human respiratory system from sulfur dioxide.

References

[1] S.J. Allen, E. Ivanova, B. Koumanova, *Chem. Eng. J.* 152(2-3) (2009) 389-395.
[2] G.J. Kubas, *Inorg. Chem*. 18(1) (1979) 182-188.
[3] D. Hua, Y. Honghong, T. Xiaolong, L. Haiyan, Z. Xuan, *Exch. Zeolites* 52(20) (2013) 6778-6784.
[4] A. Gupta, V. Gaur, N. Verma, *Chem. Eng. Process.* 43(1) (2004) 9-22.
[5] M.A. Hanif, N. Ibrahim, A. Abdul Jalil, *Environ. Sci. Pollut. Res*. 27(22) (2020) 27515-27540.
[6] Y. Boutillara, J.L. Tombeur, G. De Weireld, P. Lodewyckx, *Chem. Eng. J.* 372 (2019) 631-637.
[7] Y. Zhou, M.Z. Cai, X.J. Shu, Z.H. Xu, L.S. Zhou, X. Wu , *Chem. Eng. J.* 435 (2020) 134876.
[8] W. Li, J. Li, T.D. Duong, S.A. Sapchenko, X. Han, J.D. Humby, S. Yang, *J. Am. Chem. Soc*. 144(29) (2022) 13196-13204.
[9] H.C. Lan, Y.T. Zou, Y.C. Wang, N. N. Cheng, W. L. Xu, H.L. Peng, J. Du, *Chem. Eng. J.* 422 (2021) 129699.
[10] H. Deng, H. Yi, X. Tang, H. Liu, X. Zhou, *Ind. Eng. Chem. Res.* 52(20) (2013) 6778-6784.
[11] T. Rakitskaya, T. Kiose, L. Raskola, *Chem. J. Moldova* 16(2) (2021) 91-101.

[12] T.L. Rakitskaya, T.A. Kiose, L.A. Raskola, K.O. Golubchik, A.B. Shulga, A.P. Nazar, A.A. Stoyan, *Visn. Odes. Nats. Univ., Khim.* 23(2) (2018) 6-17.
[13] T.L. Rakitskaya, T.A. Kiose, V.O. Vasylechko, V.Ya. Volkova, G.V. Gryshhouk, *Chem. Met. Alloys* 4(3-4) (2011) 213-218.
[14] M.N.J. Treacy, J.B. Higgins *Collection of Simulated XRD Powder Patterns for Zeolites*, Amsterdam: Elsevier, 2001. 586 p.
[15] A. Nazar, T. Rakitskaya, T. Kiose, *Chem. J. Moldova* 17(1) (2022) 47-55.
[16] J.M. Anast, D.W. Margerum*, Inorg. Chem*. 20(7) (1981) 2319-2326.
[17] I. Grgić, V. Hudnik, M. Bizjak, J. Levec, *Atmos. Environ*. *A* 25(8) (1991) 1591-1597.
[18] C. Brandt, I. Fabifin, R. Eldik, *Inorg. Chem*. 33(4) (1994) 687-701.
[19] S. Luňák, A.M. El-Wakil, J. Vepřek-Šiška, *Collect. Czech. Chem. Commun.* 43(12) (1978) 3306-3316.
[20] R.K. Ulrich, G.T. Rochelle, R.E. Prada, *Chem. Eng. Sci.* 41(8) (1986) 2183-2191.
[21] M.K. Doula, A. Ioannou, *Microporous Mesoporous Mater*. 58(2) (2003) 115-130.
[22] T.L. Rakitskaya, A.S. Truba, T.A. Kiose, L.A. Raskola, *Visn. Odes. Nats. Univ., Khim.* 20(2) (2015) 27-48.
[23] T.L. Rakitskaya, V.O. Vasylechko, T.A. Kiose, G.V. Gryshchouk, A.M. Dzhiga, V.Y. Volkova, *Chem. Met. Alloys* 8(1-2) (2015) 32-38.
[24] T. Kiose, T. Rakitskaya, A. Ennan, V. Vasylechko, G. Gryshchouk, *Chem. Chem. Technol*. 17(2) (2023) 272-278.